Postprint Version

N. J. Shirtcliffe, S. Aqil, C. Evans, G. McHale, M. I. Newton, C. C. Perry, P. Roach, *The use of high aspect ratio photoresist (SU8) for super-hydrophobic pattern prototypes*, J. Micromech. Microeng. 14 (10) (2004) 1384-1389; DOI:10.1088/0960-1317/14/10/013.

The use of high aspect ratio photoresist (SU-8) for super-hydrophobic pattern prototyping

Neil J. Shirtcliffe*, Sanaa Aqil, Carl Evans, Glen McHale,

Michael I. Newton, Carole. C. Perry, Paul Roach

School of Science,

The Nottingham Trent University,

Clifton Lane,

Nottingham NG11 8NS, UK

Abstract

In this work we present a reliable technique for the production of large areas of high aspect ratio patterns and their use as model super-hydrophobic systems. The high thickness and straight sidewalls possible with SU-8 were used to generate dense patterns of small pillars. The photoresist patterns could be used directly, without the need for micromoulding. A method is given allowing resist thickness to be varied over a wide range and a bottom antireflective layer was used to ease patterning on reflective substrates. This patterning technique allows rapid testing of wetting theories, as pattern size and depth can be varied simply and samples can be produced in sufficient numbers for laboratory use. We show how the static contact angle of water varies with pattern height for one sample-pattern and how static and dynamic contact angles vary with dimension using high aspect-ratio patterns.

* Corresponding author: email: neil.shirtcliffe@ntu.ac.uk; Tel: +44 (0) 115 8486375; Fax: +44 (0) 115 8486636

1. Introduction

SU-8 is a negative photoresist that can be used to fabricate thick patterns with smooth walls; it is epoxy based and becomes strong, stiff and chemically resistant after processing. The resist can be removed in severe conditions and has shown some utility in this aspect [1] but its main strength is that it can be left in the device e.g. as wave guides [2, 3] and even used structurally e.g. in MEMS devices [4, 5, 6]. SU-8 is also used in larger scale patterns in microfluidics as very thick structures can be produced and bonded together [7, 8]. Negative sidewalls or T-topping, producing mushroom shaped pillars can a problem with this resist, but this effect can be utilised in some devices [9]. Much of the work done using SU-8 has involved relatively large-scale patterns (>50 μm) but finer patterns with high aspect ratio have also been produced [10].

The properties of SU-8 also make it suitable for making super-hydrophobic surfaces; these can take the form of arrays of pillars with separations of less than 50 μm. Super-hydrophobic surfaces are hydrophobic surfaces with high surface roughness. The combination reduces interaction between water and the surface and can allow drops to roll off surfaces that are slightly inclined. This potentially useful effect has often been observed on surfaces that are difficult to model; the use of SU-8 has allowed well-defined surfaces to be designed and their super-hydrophobicity tested.

Recent studies into super-hydrophobic surfaces were started in 1996 with a surface obtained using the crystallisation of alkylketene dimer (AKD) to provide a fractally rough surface [11, 12]. Since that time super-hydrophobic surfaces have been obtained using glass beads [13], the sol-gel process [14, 15], vacuum deposited PTFE thin films [16, 17], anodic oxidation of aluminium surfaces [12] and plasma-polymerisation [18, 19] amongst others. In many of these cases the idea has been to create a high aspect ratio topographic surface and then to apply a thin (~monolayer) hydrophobic coating.

More recently, lithographic patterning of silicon wafers has been used to create regular, high aspect-ratio patterns [20] with the aim of creating simple models to investigate the phenomenon. Yoshimitzu *et al* [21] sawed patterns into silicon wafers with a wafer saw, which is simpler than lithography but is limited to relatively large patterns and sawn faces tend to be grooved. Super-hydrophobic surfaces have also been created with photoresist previously with Kawai and Nagata [22] preparing rough surfaces using photoresist patterns of up to 2 μm in height and aspect ratios up to 1.2. They did not attempt to alter the chemistry of the surfaces of these patterns but did show contact angle changes with pattern height. Recently He *et al* [23] produced super-hydrophobic surfaces using PDMS moulds of SU-8 photoresist patterns. Their aspect ratio, however, was not very high (<0.4 for some patterns); it is possible that they did not reach the highest possible contact angle for their pattern geometry.

This paper describes how patterning thick photoresist and treating it with a cheap and easily available hydrophobic coating can produce super-hydrophobic test patterns. The patterns developed had feature sizes from 4 to 40 μm, aspect ratios of up to 7 and could be produced with quite smooth sides. Using SU-8, photolithographic

patterns can cover large areas of most materials, limited only by mask dimensions. The pattern could be varied across the sample to produce gradients in super-hydrophobicity, potentially allowing drops to be steered across surfaces.

2. Method

Patterns were prepared using SU-8 50 from Microposit; most samples were prepared on 18 mm square borosilicate glass coverslips (18 mm square, Menzel). These were cleaned by sonication in Decon 90 (Decon) followed by ethanol (Fischer p.a.). A mask was used with a pattern of open circles spaced in a square array with the spaces between the nearest neighbours being equal to the diameter of the circles. Because SU-8 is a negative resist a pattern of round pillars was produced. A range of pillar diameters was tested from 2 to 40 μm.

2.1 SU-8 processing notes

SU-8 50 (Microposit) can be diluted using its developer, PGMEA (1-methoxy 2-propyl acetate, Aldrich). It was found necessary to filter the solvent though a 0.2 μm syringe filter (Whatmann, PTFE) before use. The mixture was warmed to 40º C to reduce viscosity and aid mixing and was shaken or stirred, depending on the viscosity. The diluted SU-8 was allowed to stand overnight before use to ensure that it was thoroughly mixed. Diluted SU-8 50 was used to produce thin layers of SU-8. It was found that the layers were flatter, with consistently smaller edge beads at any given thickness if the spinning speed was kept high (4000-6000 rpm).

Reflective samples (gold) were first coated with an anti-reflective layer. Thick resists transmit quite a large proportion of the UV light used to expose them and any reaching the gold would be reflected back through the resist. If the incident beam is not parallel or the gold is not planar the reflected beam will spread, leading to patterns with larger tops than bottoms. Thin layers of anti-reflective materials can prevent this. After cleaning the substrates XHRiC-16 (Brewer science USA) was spun onto the samples using two-stages, 500 rpm for 5 s then 3500 rpm for 30 s; accelerating at 100 rpm s^{-1} in both cases. The anti-reflective layer was baked on a hotplate at 230 ºC for 80 s. The XHRiC-16 was then coated with a protective layer to prevent the SU-8 and anti-reflective layer from mixing. Omnicoat (MicroChem USA) was used for this purpose and was applied using the same spinning and baking cycle as the XHRiC-16.

Glass and silicon samples were dried by heating them to 220 ºC on a hotplate for 10 min; they were then transferred to a level, cool surface. SU-8 was poured on and spread out using a glass rod or applied using a Pasteur pipette, depending on its viscosity. Samples were then covered and left to stand for 15 min to allow bubbles in the SU-8 to escape. The cover was used to reduce the rate of solvent evaporation.

Spinning was carried out on an Electronic Micro Systems 4000 spin coater in a fume-cupboard; the chuck was accelerated to 400 rpm at 100 rpm s^{-1} and held for 10s before being accelerated to the final speed at 100 rpm s^{-1} and held at this speed for 45-60 s. Final speeds ranged from 2000 to 6000 rpm.

SU-8 layers were pre-baked on a hotplate for 1 m at 65 ºC followed by 20 min at 95 ºC. This was sufficient for all thicknesses up to 60 μm, greater thicknesses required longer times at the higher temperature. Samples were then allowed to cool for 10 min reaching room temperature in this time.

Exposure was carried out using a Cobilt C-800 mask aligner. Exposure doses published by Microchem inc. were found to be close to optimal except for on smooth, reflective surfaces. The use of an anti-reflective bottom coat allowed all samples to be treated as non-reflective. A filter, cutting out wavelengths shorter than 250 nm, was required to avoid concave profiles. A sheet of ¾ C.T. blue filter (Lee filters UK) was used for this purpose, which also reduced the I-line intensity of the source.

Post-exposure-baking was carried out on a hotplate; the same profile was used for thicknesses from 3 to 60 μm. The hotplate was levelled and situated away from draughts, samples were placed on the hotplate at room temperature, and the temperature was then increased to 55 ºC and held for 10 min; it was then increased to 70 ºC and held for a further 10 min; then it was raised to 95 ºC for 5 min and finally to 110 ºC for 20 min. After the final heating stage the power was switched off and the hotplate and samples allowed to cool undisturbed for at least 2 h. It was found that slow cooling improved the adhesion of SU-8 to the substrate.

Arrays of thin pillars are difficult to prepare by photolithography as development can cause them to bend, break or lift off [24]. Tanaka *et al* [25] calculated that an aspect ratio of 5 cannot easily be exceeded if water is the solvent drying (surface tension 72.28 dyn cm^{-1}). During drying the surface tension at the top of the pattern acts to pivot the individual sections towards one another. For pillar patterns the diameter of the pillars will determine their strength and the distance between them the strength of the attractive force. The force increases with the reciprocal of the distance between the pillars. The thin, closely spaced pillar forests that show super-hydrophobicity are therefore likely to be affected. Reducing the surface tension and increasing the contact angle of the last solution used to wash the samples can reduce the force on the pattern during drying and thus prevent pattern collapse. Samples prepared for this study were developed in PGMEA as usual and then rinsed with acetone (Fischer p.a.) before being placed into a beaker of diethyl ether (Fischer p.a.) for 2 min to ensure that the pattern was filled with ether. Diethyl ether has a low surface tension (17.06 dyn cm^{-1}) so the forces on the pattern during drying were low. Elimination of the effect was possible by washing with methanol instead of diethyl ether and exchanging this for liquid carbon dioxide under pressure before removing this above its supercritical point. This was found not to be necessary for the patterns produced for this paper but should prove useful when extending the aspect ratio range.

Kawai *et al* [26] show that the peeling strength of photoresist films is broadly dependent upon the baking temperature. Unfortunately the minimum peel strength of resists coincides with the post-exposure baking temperature of SU-8. As it is not possible to increase the baking temperature of SU-8 above 135 ºC lower temperatures might be more successful, but our results suggest that SU-8 adhesion falls below 100º C. Kawai *et al.* [26] go on to suggest that hydrogen bonding plays a major part in resist adhesion, which explains why drying and temperatures above 100 ºC are important.

2.2 Surface treatment

The contact angle of water on flat, cured, SU-8 is just under 80º. To increase this the patterns were treated with a wash in solution designed for waterproofing breathable fabrics (Grangers Extreme Wash In). These preparations consist of

fluorocarbons emulsified in water with a detergent. The agent was diluted in deionised water by a factor of 50 and the samples immersed at room temperature for 20 min. They were then removed and gently rinsed in deionised water before being blown dry with nitrogen. The surfactants in the coating were removed by heating the samples to 40 ºC for 20 h in a drying oven. This treatment was found to coat this particular type of sample evenly, as far as we could detect by electron microscopy, and increased the contact angle to around 115º.

2.3 Characterisation

Scanning electron microscope measurements were carried out on gold-coated samples using a Jeol JSM-840A with an acceleration voltage of 10 kV.

Contact angle measurements were made by taking images of water drops using a Krüss DSA10. 1 µl of deionised water was dropped onto the sample from a hydrophobised needle on a microsyringe. The needle usually had to be tapped to get the drop to detach. A picture of the drop was taken a few seconds later, to avoid any problems related to drying of the drop. The drop shapes were found to be often uneven, so tangent measurements were made and three images (six angles) were taken to allow removal of the occasional rogue point, caused by contamination of the surface. Advancing and receding angles were measured by placing a 3.5 µl drop onto a tilting stage and filming the drop at 10 frames per second as the tilt angle perpendicular to the camera was increased. Advancing and receding angles were taken as the front and rear angles on the last frame before the drop started to move.

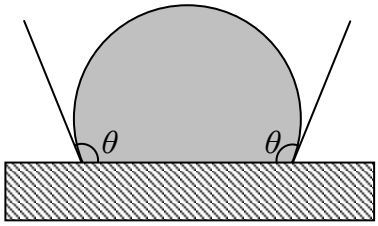

Figure 1 Diagram of a drop on a surface showing the contact angle, θ.

3. Super-hydrophobicity theory

Small drops of water on surfaces form equilibrium shapes that minimise surface energy. The minimum water-air interfacial area occurs when the drop forms a hemisphere on the surface. Positive or negative energy contributions from changing solid-air interface to solid-liquid interface cause the drop to flatten out or roll up more, increasing the water-air interface but reducing the total interfacial energy. Small drops maintain a shape that is part of a sphere, known as a spherical cap. A convenient way to describe these shapes is the angle between the water-liquid interface and the solid-liquid interface where they intersect, the contact angle (figure 1).[27, 28, 29]. Materials with a low surface energy produce high water contact angles, and the greatest are observed on perfluorocarbons and approach 120º. The contact angle can be increased above this by making the solid surface rough. This increases the specific surface energy cost of creating solid-liquid interface. Wenzel [30] described this theoretically, suggesting that the contact angle could approach 180°. Figure 2 shows examples of photographs of the sides of water drops on hydrophilic (*a*), hydrophobic (*b*) and super-hydrophobic (*c*) surfaces.

Wenzel's equation predicts that the basic wetting behaviour of a surface will be enhanced by roughness so that creating roughness on a flat surface with an equilibrium contact-angle $\theta_{e(flat)}$>90° will increase the contact angle. In practice, intimate contact is not usually maintained between liquid and solid on very rough surfaces with $\theta_{e(flat)}$>90°. The liquid drop, therefore, effectively sits upon a composite surface of the peaks of the topography and the air separating the surface features and Cassie and Baxter's equation [31] applies instead of Wenzel's. Nonetheless, the contact angle is still increased. One of the key differences to the predictions from Wenzel's equation is that the effect of roughness on a surface further emphasises super-hydrophobicity, with the critical contact angle for which roughness causes increased apparent contact angle reduced to below 90°. A second difference is that a droplet obeying a Cassie-Baxter equation can easily be moved across the surface whereas one obeying the Wenzel equation cannot.

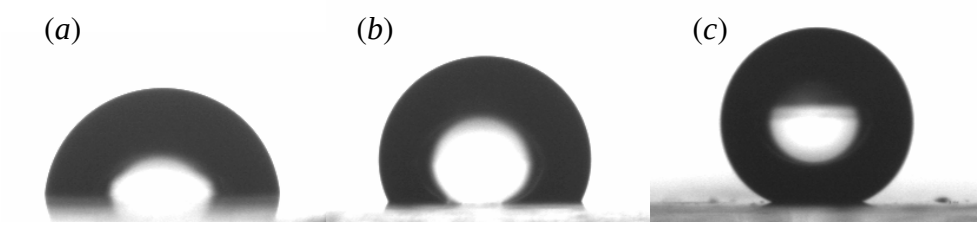

Figure 2. Photographs of water drops on different surfaces (*a*) flat, hydrophilic surface (SU-8) contact angle = 80º; (*b*) flat, hydrophobic surface (Grangers treated a) contact angle = 115º; (*c*) Hydrophobised SU-8 pattern contact angle = 155º.

3.1 Advancing and receding angles

When a surface with a drop on it is tilted the drop sags towards the lower side; the contact angle on the lower side increases and that on the upper side decreases. When they reach certain boundary values the drop begins to move, these are known as the advancing and receding angles (Figure 3). If the difference between the advancing and receding angles is low (low contact angle hysteresis) the drop will roll off the surface at low tilt angles.

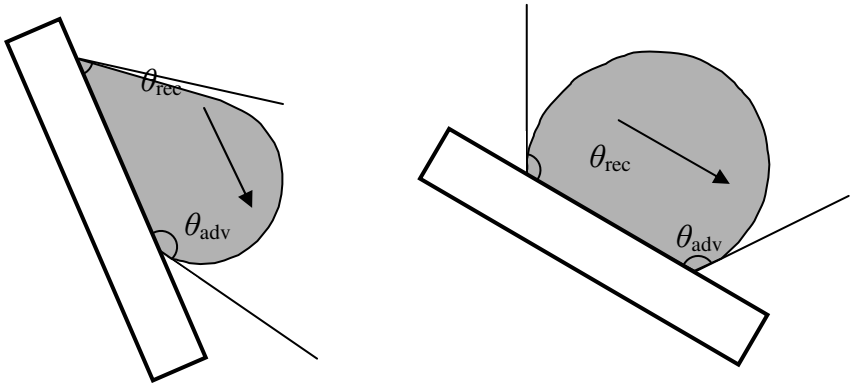

Figure 3. Advancing and receding angles on drops just moving on tilted surfaces, the surface on the right shows lower contact angle hysteresis than that on the left.

Öner and McCarthy [20] suggest that the contact angle hysteresis or the tilt angle required for drop motion should be included in the definition of super-hydrophobicity as this determines whether water will remain on a surface or not.

4. Results

4.1 Range of samples available

Patterns were prepared with thicknesses up to 80 μm and aspect ratios of up to 7. Below 7 μm diameter the patterns became more difficult to produce and patterns below 4 μm were generally unsuccessful. The mask used was divided into 12 ×12 mm sections of each pattern size but experiments with wafers showed that the pattern area was only limited by the size of the mask aligner. Dilution with PGMEA allowed the thickness of the patterns to be varied down to below 1 μm. This allowed patterns of a large range of aspect ratios to be generated. Figure 4 shows the range of patterns that could be produced.

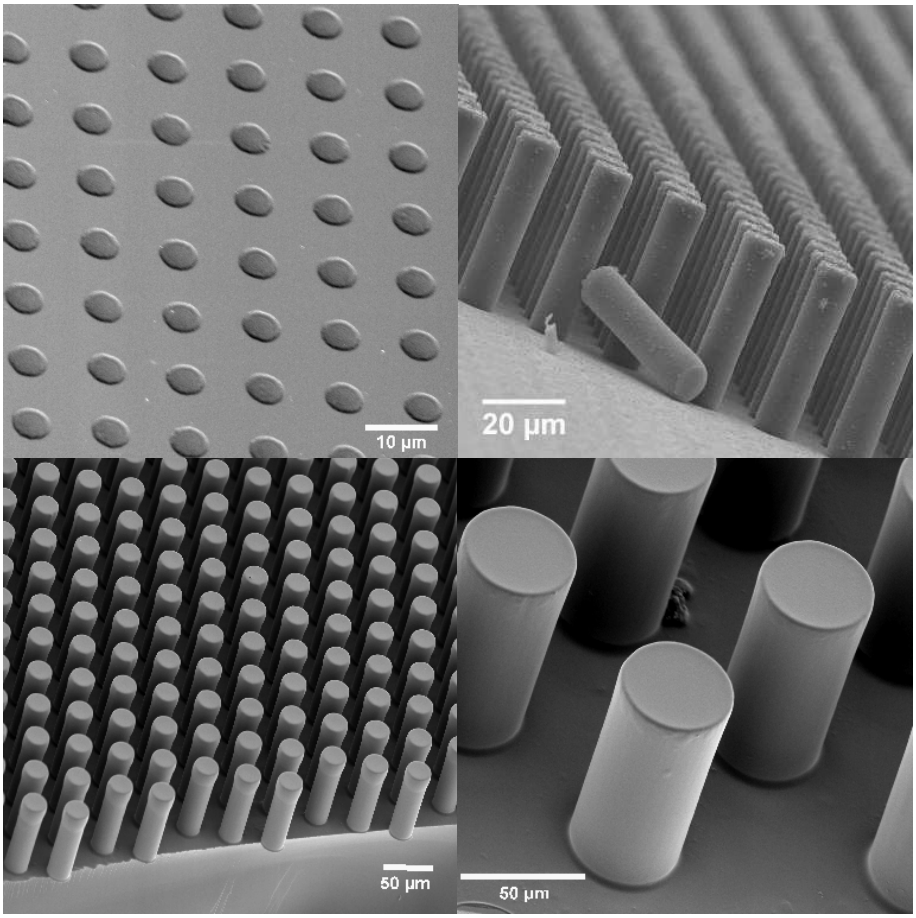

Figure 4. Patterned SU-8 surfaces, circular pillars of various heights and diameters in square patterns.

4.2 Varying pattern height

15 μm diameter pillar patterns of varying heights were produced and the contact angle of water upon them was measured. As shown in Figure 5(*a*) and (*b*) the equilibrium contact angle increased as the pattern height (aspect ratio) was increased and reached a maximum of 145º when the samples were hydrophobised and 143º when they were not. The minimum height for saturation to occur on this pattern was about 15 μm, an aspect ratio of 1, whether or not they were hydrophobized.

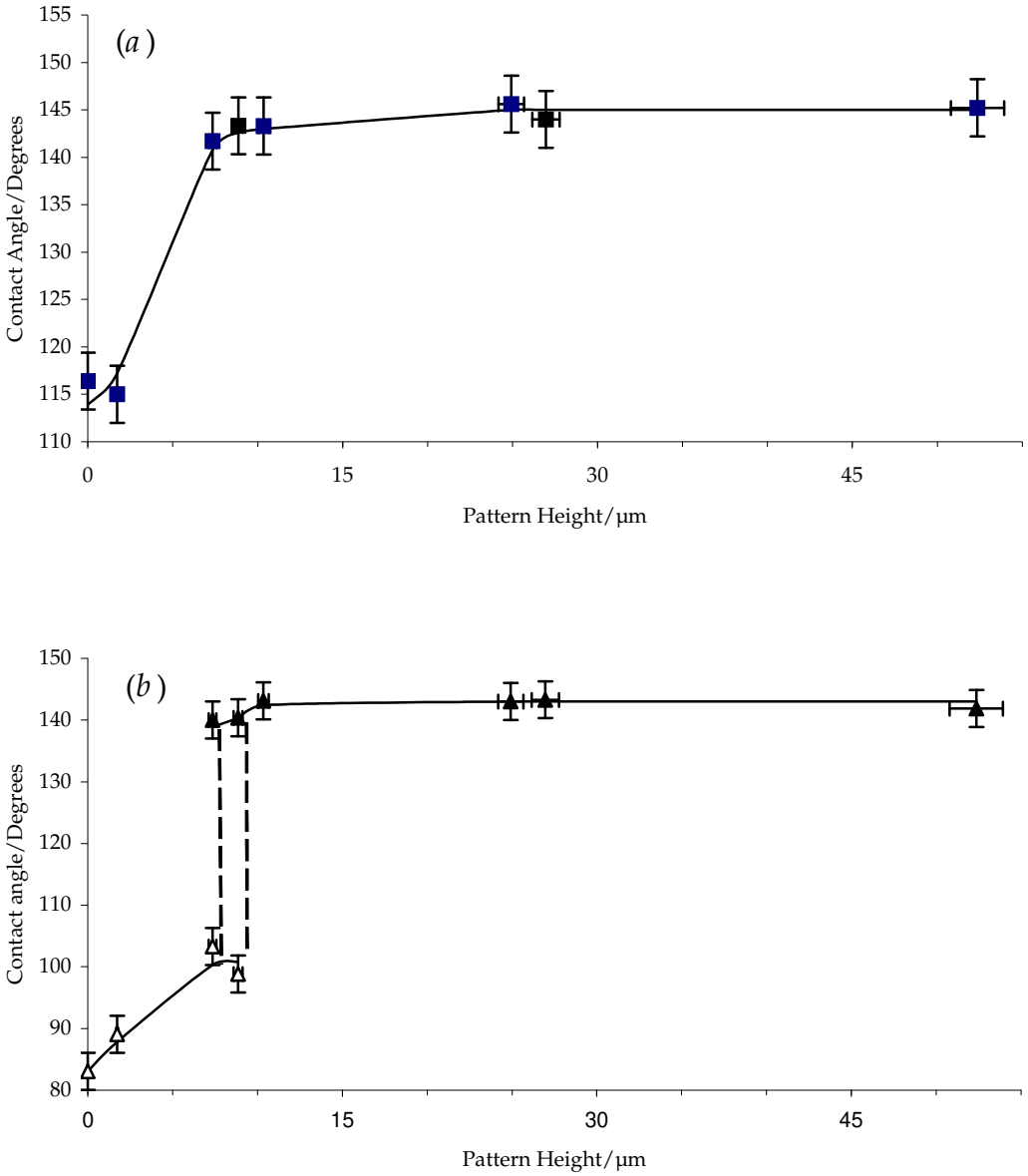

Figure 5. Change in contact angle as the height of 15 μm pillars showing the contact angles on both untreated and treated surfaces; (*a*) surface treated with fluorocarbon, (b) the untreated surface.

Using Cassie and Baxter's formula equation (1) [32], assuming that the drops only contact the tops of the pillars when the contact angle has reached its maximum, contact angles of 140.3º uncoated and 152.4º coated would be expected.

$$\cos\theta_r = f_1 \cos\theta_s - (1 - f_1) \tag{1}$$

where θ_r is the contact angle on the rough surface, θ_s that on a smooth surface of the same type and f_1 the fraction of the surface contacted by the drop. For the patterns used here a circle of area πr^2 was in contact with the drop and the area of a unit cell of the pattern was a square of area $(4r)^2$, giving a value for f_1 of $\pi/16$.

The difference between these calculated and measured angles reflects the contact angle hysteresis on these surfaces, which makes measurement of true equilibrium angles difficult. The measured equilibrium angles should really be called quasi-equilibrium angles.

In Figure 5(*b*) two contact angles were observed on samples of heights around 10 μm, depending upon whether the drop was forced down onto the pattern or carefully placed. This shows that the drop can either bridge the roughness or wet the whole sample, that the Wenzel angle is lower and that the energy barrier between these minima is not great. Bico *et al* [33] and Suzuki *et al* [34] have shown that this can occur as long as the aspect ratio of the pattern is not great.

4.3 Varying pattern size

Equilibrium, advancing and receding contact angles of a series of patterns of different sizes were measured, with the pattern unit cell geometry remaining constant, but varying the size. The aspect ratio of the patterns was maintained above 2 to ensure that the contact angle was at its maximum, Cassie-Baxter, value. This meant that 5 μm patterns were >10 μm high and 40 μm > 80 μm. The results are displayed in Table 1 and suggest that there is no influence of pattern dimension on any of these angles.

Table 1. Advancing and receding angles on high aspect ratio patterns of circular pillars with spacings equal to their diameter varying the diameter and spacing together.

Pillar diameter (μm)	Equilibrium CA (±3°)	Advancing CA (±4°)	Receding CA (±34°)
5	147	154	100
15	145	152	99
25	146	153	105
30	147	153	100
40	145	152	97

McCarthy *et al*. [20] used triangular patterns of circular pillars and reported no changes in static, advancing or receding contact angle below 32 μm pillar-spacing as seen here. However, they also used different shapes of pillar to show that the receding angle decreased if the perimeter of the pillars increased. This led them to the conclusion that the receding angle should be dependent upon the strength of contact line pinning on the surface. Extrand [35] also considered the length of the contact line and predicted increases in advancing and receding contact angles with increasing perimeter.

The perimeter of the top of a circular pillar of radius r is $2\pi r$, the pattern used has one circular pillar per square of side $4r$. A unit square will contain $1/(4r)^2$ of these unit cells so the perimeter of the tops of the pillars per unit area will be $2\pi r/16r^2 = \pi/8r$. This means that the perimeter of the pattern decreases with the reciprocal of r so on decreasing the pattern from 40 μm to 5 μm the perimeter will increase by a factor of 8. This change in specific perimeter had no measurable effect on the receding angle. This suggests that corners or indented edges may have influenced McCarthy *et al*'s results and that the contact area below circular pillars may determine contact angle hysteresis.

5. Conclusion

Test super-hydrophobic patterns were successfully produced using thick photoresist. The resist was mechanically stable enough to suspend drops of water and could be used uncoated or coated to investigate different flat contact angles. The aspect ratio of the patterns could be made sufficiently great so that the contact angles saturated at a high value with the value calculated from Cassie and Baxter's equation (1) occurring between the measured advancing and receding angles.

Superhydrophobic SU-8 patterns show promise for use in micro-fluidic devices as SU-8 was patterned on silicon, silica and metals with the use of an antireflective layer and pattern area is potentially only limited by mask dimensions. SU-8 is already used in some devices and the addition of super-hydrophobicity may improve some of them.

Varying the dimensions of the pattern of circular pillars changed the length of the contact perimeter without changing the contact area. No changes in contact angles or contact angle hysteresis were observed. The equilibrium contact angle would be expected to remain constant as the value of f_1 in the Cassie-Baxter equation (equation (1)) is constant. The unchanging contact angle hysteresis, however, disagrees with some wetting theories and shows how the technique could be used to systematically investigate other theories, such as Patankar's [36] method for designing hydrophobic surfaces.

Acknowledgement

The authors acknowledge the financial support of the UK EPSRC and MOD/Dstl (Grants GR/R02184/01 and GR/ GR/S34168/01).

[1] Son, S., Park, Y., Choi, S., 2002, New formation technology for a plasma display panel barrier-rib structure using a precise metal mold fabricated by the UV-LIGA process, *J. Micromech. Microeng.* **12** 63-69.

[2] Nathan, M., Levy, O., Goldfarb, I., Ruzin, A., 2003, Monolithic coupling of a SU8 waveguide to a silicon photodiode, *J. Appl. Phys.* **94** 7932-7934.

[3] Elgaid, K., McCloy, D., Thayne, I., 2003, Micromachined SU8 negative resist for MMIC applications on low resistivity CMOS substrates, *Microelect. Eng.* **67-8** 417-421.

[4] Seidemann, V., Rabe, J., Feldmann, M., Buttgenbach, S., 2002, SU8-micromechanical structures with in situ fabricated movable parts, *Microsyst. Tech.* **8** 348-350.

[5] Houlet, L., Helin, P., Bourourina, T., Reyne, G., Dufour-Gergam, E., Fujita, H., 2002, Movable vertical mirror arrays for optical microswitch matrixes and their electromagnetic actuation, *IEEE J. Sel. Quantum Electron.* **8** 58-63.

[6] McNie, M., King, D., Vizard, C., Holmes, A., Lee, K., 2000, High aspect ratio micromachining (HARM) technologies for microinertial devices, *Microsyst. Technol.* **6** 184-188.

[7] Lin, C. Lee, G. Chang, B., Chang, G., 2002, A new fabrication process for ultra-thick microfluidic microstructures utilizing SU-8 photoresist, *J. Micromech. Microeng.* **12** 590-597.

[8] Griscom, L. Degenaar, P., Lepioufle, B., Tamiya, E., Fujita, H., 2001, Cell placement and neural guidance using a three-dimensional microfluidic array, *Jap. J. Appl. Phys.* 1 **40** 5485-5490.

[9] Kabseog, Kim, Park, D., Hong, Lu, Wooseong, Che, Kyunghwan, Kim, Jeong-Bong, Lee, Chong, Ahn, 2004, A tapered hollow metallic microneedle array using backside exposure of SU-8, *J. Micromech. Microeng.* **14** 597-603.

[10] Malek, C., 2002, SU8 resist for low-cost X-ray patterning of high-resolution, high-aspect-ratio MEMS, *Microelec. J.* **33** 101-105.

[11] Onda, T., Shibuichi, S., Satoh, N., Tsujii, 1996, K., Super-water-repellent fractal surfaces, *Langmuir* **12** 2125-2127.

[12] Shibuichi, S., Yamamoto T., Onda T., Tsujii K., 1996, Super water-repellent surfaces resulting from fractal structure, *J. Phys. Chem.* **100** 19512-19517.
[13] Fuji, M., Fujimori, H., Takei, T., Watanabe, T., Chikazawa, M., 1998, Wettability of glass-bead surface modified by trimethylchlorosilane, *J. Phys. Chem.* B **102** 10498-10504.
[14] Tadanaga, K., Kitamuro, K., Matsuda, A., Minami, T., 2003, Formation of superhydrophobic alumina coating films with high transparency on polymer substrates by the sol-gel method, *J. Sol-gel Sci Technol.* **26** 705-708.
[15] Tadanaga, K., Morinaga, J., Minami, T., 2000, Formation of superhydrophobic-superhydrophilic pattern on flowerlike alumina thin film by the sol-gel method, *J. Sol-Gel Sci. Technol.* **19** 211-214.
[16] Miller, J., Veeramasuneni, J., Drelich, J., Yalamanchili, M. R., 1996, Effect of roughness as determined by atomic force microscopy on the wetting properties of PTFE thin films, *Polym. Eng. Sci.* **36** 1849-1855.
[17] Palumbo, G., D Agostino, R., Lamendola, R., Corzani, I., Favia, P., European Patents EP0985741 and EP0985740 with Procter and Gamble, 2000, Modulated plasma glow discharge treatments for making super hydrophobic substrates.
[18] Coulson, S.R., Woodward, I., Badyal, J.P.S., Brewer, S.A., Willis, C., 2000, Super-repellent composite fluoropolymer surfaces, *J. Phys. Chem.* B **104** 8836-8840.
[19] Shirtcliffe, N., Thiemann, P., Stratmann, M., Grundmeier, G., 2001, Chemical structure and morphology of thin, organo-silicon plasma-polymer films as a function of process parameters, *Surf. Coat. Technol.* **142** 1121-1128.
[20] Öner, D., McCarthy, T. J., 2000, Ultrahydrophobic surfaces. Effects of topography length scales on wettability, *Langmuir* **16** 7777-7782.
[21] Yoshimitzu, Z., Nakajima, A., Watanabe, T., Hashimoto, K., 2002, Effects of surface structure on the hydrophobicity and sliding behavior of water droplets, *Langmuir* **18** 5818-5822.
[22] Kawai, A, Nagata, H., 1994, Wetting behavior of liquid on geometrical rough surface formed by photolithography, *Jpn. J. Appl. Phys.* **33** L1283-1285.
[23] He, B., Patankar, N., Lee, J., 2003, Multiple equilibrium droplet shapes and design criterion for rough hydrophobic surfaces, *Langmuir* **19** 4999-5003.
[24] Lee, H., Park, J., Yoo, J., An, J., Oh, H., 2003, Resist pattern collapse modeling for smaller features, *J. Korean Phys. Soc.* **42** S202-S206.
[25] Tanaka, T., Morigami, M., Atoda, N., 1993, Mechanism of resist pattern collapse during development process, *Japan J. Appl. Phys.* **32** 6059-6064.
[26] Kawai, A., Nagata, H., Moromoto, H., Takata, M., 1994, Adhesion of photoresist pattern bakes at 80 to 325-degrees-C to inorganic solid-surface, *Japan J. Appl. Phys.* **33** L146-148.
[27] de Gennes P. G., 1985, Wetting – statics and dynamics, *Rev. Mod. Phys.* **57** 827-863.
[28] Léger L., Joanny J.F., 1992, Liquid spreading, *Rep. Prog. Phys.* **55** 431-486.
[29] McHale, G., Newton, M. I., 2002, Frenkel's method and the dynamic wetting of heterogeneous planar surfaces, *Colloids Surf.* A **206** 193-201.
[30] Wenzel, R. N., 1936, Resistance of solid surfaces to wetting by water, *Ind. Eng. Chem.* **28** 988.
[31] Quéré, D., 2002, Rough ideas on wetting, *Physica* A **313** 32-46.
[32] Cassie, A., Baxter, S., 1944, Wettability of porous surfaces, *Trans. Faraday Soc.* **40** 546-551.
[33] Bico, J., Tordeux, C., Quéré, D., 2001, Rough wetting, *Europhys. Lett.* **55** 214-220.
[34] Suzuki, K., Uyeda, Y., 2003, Load-carrying capacity and friction characteristics of a water droplet on hydrophobic surfaces, *Tribol. Lett.* **15** 77-82.
[35] Extrand, C., 2002, Model for contact angles and hysteresis on rough and ultraphobic surfaces, *Langmuir* **18** 7991-7999.
[36] Patankar N., 2003, On the modeling of hydrophobic contact angles on rough surfaces, *Langmuir* **19** 1249-1253.